

All-optical femtosecond switch using two-photon absorption

D. D. Yavuz

Department of Physics, University of Wisconsin at Madison, 1150 University Avenue, Madison, Wisconsin 53706, USA

(Received 23 May 2006; published 13 November 2006)

Utilizing a two-photon absorption scheme in an alkali-metal vapor cell, we suggest a technique where a strong laser beam switches off another laser beam of different wavelength in femtosecond time scales.

DOI: [10.1103/PhysRevA.74.053804](https://doi.org/10.1103/PhysRevA.74.053804)

PACS number(s): 42.65.Re, 42.50.Gy

Over the last few decades, there has been a growing interest in all-optical approaches to computing and information processing [1]. All-optical approaches do not suffer from the intrinsic slow response of electronic components and have the potential for signal routing, processing, multiplexing, and demultiplexing with speeds exceeding terahertz (THz) rates. As is the case for electronic logic gates, all-optical information processing relies on nonlinear computing elements. The most commonly investigated nonlinear optical element is an all-optical switch, where a laser beam turns another laser beam on and off. Over the last few decades several approaches for all-optical switches have been suggested and demonstrated. These include optical Kerr shutters in nonlinear crystals [2–5], approaches that utilize semiconductor waveguides and quantum well structures [6–12], interferometric approaches [13], and approaches that utilize photonic crystals and organic materials [14–17]. These approaches have successfully demonstrated picosecond-time-scale all-optical switches. However, it still remains a challenge to construct all-optical switches with switching time in the femtosecond domain.

In this paper, as an alternative to these solid state approaches, we suggest the use of an atomic vapor gas and propose a femtosecond-time-scale all-optical switch. Our proposal utilizes two-photon absorption in a three level atomic system. Noting Fig. 1, the electronic ground state of the atom, state $|a\rangle$, is coupled to state $|c\rangle$ with two laser beams, E_s and E_p . The femtosecond switching beam, E_s , is strong, and its frequency is selected such that the detuning from the intermediate state, $\Delta\omega_b$, is large when compared with the switching bandwidth. A weak probe beam, E_p , then couples the intermediate state to state $|c\rangle$. Due to the large detuning, the excitation to state $|b\rangle$ is adiabatic and this state acquires significant population only for the duration of the switching laser beam. The nonadiabatic excitation of the atom to state $|c\rangle$ then causes loss on the probe beam. Since this excitation only happens when the switching laser beam has high intensity, the probe beam, E_p , is attenuated only for the duration of the switching laser beam, E_s . The scheme of Fig. 1 is similar to two-photon absorption experiments performed in nonlinear crystals [18]. However as will be demonstrated later, our scheme requires about two orders of magnitude lower switching intensities and also allows switching speeds well into the femtosecond domain.

We proceed with the analysis of our scheme. Noting Fig. 1, we consider the interaction of two laser beams with a three level atomic system. We expand the total wave function for the atomic system as

$$|\psi\rangle = c_a(t)\exp(-j\omega_a t)|a\rangle + c_b(t)\exp(-j\omega_b t)|b\rangle + c_c(t)\exp(-j\omega_c t)|c\rangle. \quad (1)$$

Here $\hbar\omega_a$, $\hbar\omega_b$, and $\hbar\omega_c$ are the energies of the discrete states. The quantities $c_i(t)$ are the probability amplitudes of the relevant states in the interaction picture. The state vector of Eq. (1) evolves with the Hamiltonian of $\hat{H} = \hat{H}_0 - E(t)\hat{P}$ where \hat{H}_0 denotes the unperturbed Hamiltonian and \hat{P} is the dipole moment operator. We take the electric field to be a sum of two fields with slowly varying envelopes: $E(z, t) = \text{Re}[E_s(z, t)\exp(j\omega_s t - jk_s z)] + \text{Re}[E_p(z, t)\exp(j\omega_p t - jk_p z)]$. E_s is the intense femtosecond switching field and E_p is the weak field that will be switched off. We define the detuning from the intermediate state as $\Delta\omega_b = \omega_b - \omega_a - \omega_s$, and define Rabi frequencies for the laser beams $\Omega_s = E_s\mu_{ab}/\hbar$ and $\Omega_p = E_p\mu_{bc}/\hbar$. Here μ_{ab} and μ_{bc} are the dipole matrix elements for the respective transitions. Within the rotating wave approximation, the Schrödinger equation for the probability amplitudes, after a phase transformation, are

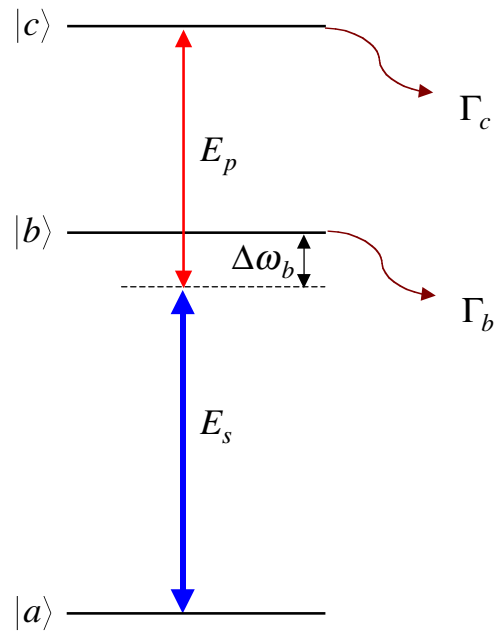


FIG. 1. (Color online) The schematic of the proposed scheme. A strong, femtosecond switching beam, E_s , couples the ground state $|a\rangle$ to the intermediate state $|b\rangle$. The nonadiabatic excitation to state $|c\rangle$ for the duration of the switching beam then causes loss on the probe beam, E_p .

$$\begin{aligned}\frac{\partial c_a}{\partial t} &= \frac{j}{2}\Omega_s c_b, \\ \frac{\partial c_b}{\partial t} + j\left(\Delta\omega_b - j\frac{\Gamma_b}{2}\right)c_b &= \frac{j}{2}\Omega_s^* c_a + \frac{j}{2}\Omega_p c_c, \\ \frac{\partial c_c}{\partial t} + \frac{\Gamma_c}{2}c_c &= \frac{j}{2}\Omega_p^* c_b.\end{aligned}\quad (2)$$

In Eq. (2), the quantities Γ_b and Γ_c denote the decay rates of states $|b\rangle$ and $|c\rangle$, respectively. The decay processes are assumed to be to states outside the system. With the probability amplitudes calculated by Eq. (2), the propagation equations for the probe and the switching beams in local time are

$$\begin{aligned}\frac{\partial\Omega_s}{\partial z} &= -\frac{j}{\hbar}\eta\omega_s N|\mu_{ab}|^2 c_a c_b^*, \\ \frac{\partial\Omega_p}{\partial z} &= -\frac{j}{\hbar}\eta\omega_p N|\mu_{bc}|^2 c_b c_c^*,\end{aligned}\quad (3)$$

where N is the atomic density and η is the impedance of free space. In Eq. (3), we have neglected the contributions of the other atomic states to the propagation of the two laser beams. We have also assumed the beams to be large in the transverse spatial dimensions and have neglected diffraction effects.

Before we proceed with a perturbative analytical solution of Eqs. (2) and (3), we first present a numerical example for a real atomic system. We take states $|a\rangle$, $|b\rangle$, and $|c\rangle$ to be $5S_{1/2}$, $5P_{3/2}$, and $4D_{5/2}$ states of ^{87}Rb . The $5S_{1/2} \rightarrow 5P_{3/2}$ transition wavelength is 780.2 nm ($D2$ line) and the $5P_{3/2} \rightarrow 4D_{5/2}$ transition wavelength is 1529.3 nm. We assume linearly polarized fields and use the values reported in Ref. [19] for the dipole matrix elements. We take the switching beam envelope to be Gaussian with a full width at half-maximum (FWHM) of 50 femtoseconds and a peak intensity of 6 GW/cm². We take $\Delta\omega_b = -500$ cm⁻¹ which is larger than

the spectral width of the switching laser and assume an atomic density of $N = 2 \times 10^{15}$ /cm³. We numerically solve Eqs. (2) and (3) on a space-time grid with the initial condition that all the atoms start in the ground state $|a\rangle$ and the boundary condition that the switching beam is a femtosecond pulse and the probe beam is monochromatic at the beginning of the vapor cell [as shown in dashed and solid lines of Fig. 2(a)].

In Fig. 2, we plot the normalized intensity of the probe beam $I_p = |E_p|^2/2\eta$ at $z=0$, $z=5$ cm, and $z=10$ cm, respectively. The normalized intensity of the switching beam $I_s = |E_s|^2/2\eta$ is also plotted (dashed line). As the probe beam propagates through the medium, it becomes switched off by the strong switching beam. The switching beam experiences about 25% drop in peak intensity due to the dispersion of the vapor gas.

In Fig. 3, we demonstrate the ability of our scheme to produce all-optical amplitude modulation at very high rates. In this simulation, we assume the switching beam to be amplitude modulated at a rate of 10 THz at the beginning of the vapor cell as shown by the dashed line in Fig. 3(a). The probe beam is again assumed to be monochromatic at the beginning of the vapor cell. The other parameters of the simulation are identical to that of Fig. 2. In Fig. 3(b), we plot the intensity of the probe beam after $z=2.5$ cm propagation through the vapor cell. The probe beam becomes amplitude modulated at a rate determined by the switching beam. The numerical simulation of Fig. 3 demonstrates that an optical data stream that is encoded into the switching laser beam can be transferred to the probe laser beam at very high rates. This opens up the possibility of wavelength division multiplexing exceeding THz rates.

We now present an analytical solution of Eqs. (2) and (3) to get an insight into the results of Figs. 2 and 3. We proceed perturbatively and assume that most of the population of the atomic system remains in the ground state and take $c_a \approx 1$. We take the probe beam, E_p , to be weak when compared with the strong switching beam, E_s . With $\Delta\omega_b$ large when

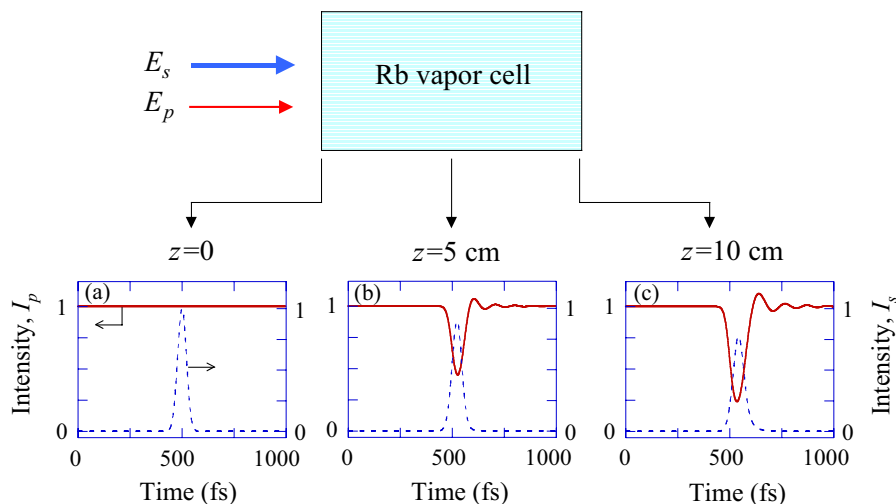


FIG. 2. (Color online) The normalized intensity of the probe beam, $I_p = |E_p|^2/2\eta$, (a) at $z=0$ cm, (b) at $z=5$ cm, and (c) at $z=10$ cm, respectively. The dashed line is the normalized intensity of the switching beam $I_s = |E_s|^2/2\eta$. As the probe beam, E_p , propagates through the medium, it becomes switched off by the strong switching beam.

compared with the spectral width of the femtosecond switching pulse, we can adiabatically eliminate the derivative of probability amplitude of state $|b\rangle$, and the perturbative solution of Eq. (2) is

$$c_b(z,t) = \frac{\Omega_s^*(z,t)}{2\left(\Delta\omega_b - j\frac{\Gamma_b}{2}\right)},$$

$$c_c(z,t) = \frac{j}{2}\exp\left(-\frac{\Gamma_c}{2}t\right)\int_0^t \Omega_p^*(z,t')c_b(z,t')\exp\left(\frac{\Gamma_c}{2}t'\right)dt'. \quad (4)$$

With the above perturbative solution, the propagation equation for the probe beam [Eq. (3)] becomes

$$\begin{aligned} \frac{\partial\Omega_p(z,t)}{\partial z} = & -\frac{\eta\omega_p N|\mu_{bc}|^2}{8\hbar\left(\Delta\omega_b^2 + \frac{\Gamma_b^2}{4}\right)}\exp\left(-\frac{\Gamma_c}{2}t\right) \\ & \times \Omega_s^*(z,t)\int_0^t \Omega_p(z,t')\Omega_s(z,t')\exp\left(\frac{\Gamma_c}{2}t'\right)dt'. \end{aligned} \quad (5)$$

To facilitate an analytical solution of Eq. (5), we make the following assumptions and simplifications: (1) We take the decay rates of the atomic states to be small when compared with the inverse of the switching time scale, $\Gamma_c t \ll 1$. (2) We take the probe beam to be monochromatic at $z=0$ and seek a solution of Eq. (5) near the beginning of the cell, $z \approx 0$, where the probe beam is not attenuated significantly. This allows us to approximate $\int_0^t \Omega_p(z,t')\Omega_s(z,t')dt' \approx \Omega_p(z,t)\int_0^t \Omega_s(z,t')dt'$ on the right-hand side of Eq. (5). (3) We assume that the switching beam is strong enough such that it remains unchanged as it propagates through the atomic medium, $\Omega_s(z,t) = \Omega_s(z=0,t)$. With these assumptions, the solution of Eq. (5) is

$$\begin{aligned} \Omega_p(z,t) &= \Omega_p(0,t)\exp[-N\sigma(t)z/2], \\ \sigma(t) &= \frac{\eta\omega_p|\mu_{bc}|^2}{4\hbar\Delta\omega_b^2}\Omega_s^*(0,t)\int_0^t \Omega_s(0,t')dt'. \end{aligned} \quad (6)$$

Here $\sigma(t)$ is the time-dependent absorption cross section for

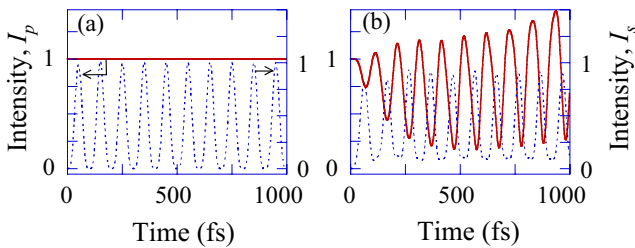


FIG. 3. (Color online) The normalized intensity of the probe beam, I_p , (a) at $z=0$ cm, and (b) at $z=2.5$ cm, respectively. The dashed line is the normalized intensity of the switching beam, I_s . The probe beam becomes amplitude modulated at a rate determined by the strong switching beam.

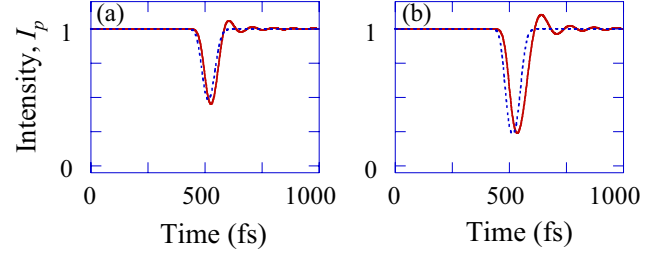


FIG. 4. (Color online) The normalized intensity of the probe beam, I_p , (a) at $z=5$ cm, (b) at $z=10$ cm, respectively, from the numerical simulation of Fig. 2. The dashed lines are the intensity profiles calculated by the analytical solution of Eq. (6). The agreement between the exact numerical results is reasonably good for both cases.

the probe laser beam. The solution of Eq. (6) is intuitive. As it propagates through the medium, the probe beam is attenuated for times only when the quantity $\Omega_s^*(0,t)\int_0^t \Omega_s(0,t')dt'$ has substantial amplitude. In Fig. 4, we plot the normalized intensity of the probe beam for the numerical simulation of Fig. 2 (solid line), together with the analytical solution of Eq. (6) (dashed line) at $z=5$ cm and $z=10$ cm. The agreement between the analytical solution and the numerical calculation is good for both cases.

The analytical solution of Eq. (6) allows for a simple estimate of the required intensity and density length product for our scheme. For a switching laser pulse with a Gaussian temporal envelope, we can evaluate the quantity $\Omega_s^*(0,t)\int_0^t \Omega_s(0,t')dt'$. The absorption cross section $\sigma(t)$ at the peak of the switching laser pulse is then

$$\begin{aligned} \sigma_{\max} &= \frac{\sqrt{\pi}}{8\sqrt{2}\ln(2)}\frac{\eta\omega_p|\mu_{bc}|^2}{\hbar\Delta\omega_b^2}|\Omega_{s,\max}|^2\tau_s \\ &= \frac{\sqrt{\pi}}{4\sqrt{2}\ln(2)}\frac{\eta^2\omega_p|\mu_{bc}|^2|\mu_{ab}|^2}{\hbar^3\Delta\omega_b^2}I_{s,\max}\tau_s. \end{aligned} \quad (7)$$

Here, the quantities $I_{s,\max}$ and τ_s denote the peak intensity and the FWHM temporal width of the switching laser pulse, respectively. For the simulation parameters of Fig. 2, the peak absorption coefficient from Eq. (7) is $\sigma_{\max} = 6.0 \times 10^{-17}$ cm². High contrast switching requires $N\sigma_{\max}L \approx 1$ where L is the length of the atomic vapor cell. For the numerical simulation of Fig. 2, this quantity is $N\sigma_{\max}L = 1.20$. For fixed $I_{s,\max}$ and τ_s , the absorption cross section, σ_{\max} , drops quadratically as the intermediate state detuning, $\Delta\omega_b$, is increased.

We now ask the question: What is the shortest switching time can one obtain using our scheme? For our scheme, it is critical that the excitation of state $|b\rangle$ is adiabatic such that the population of this state follows the intensity of the strong switching laser pulse. Adiabaticity requires the detuning, $\Delta\omega_b$, to be large when compared with the spectral width of the switching pulse. Using Eq. (7), for a fixed density-length product of the atomic medium, the required switching laser intensity scales as $I_{s,\max} \propto 1/\tau_s^3$. In Fig. 5 we plot the peak intensity of the switching beam that is required to achieve a performance comparable to the results of Fig. 2 as a function

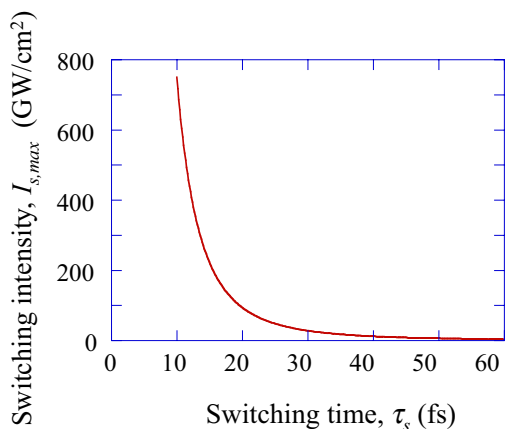


FIG. 5. (Color online) The required peak intensity of the switching beam as a function of the switching time which will give the same performance as the numerical simulation of Fig. 2. A switching time of 10 fs requires a peak intensity of about 750 GW/cm². Below 10 fs, the slowly varying envelope approximation starts to break down and the formalism of this paper is no longer valid.

of the switching time, τ_s . Switching time of 10 fs requires peak intensities of about 750 GW/cm² which is achievable with current laser technologies. Below 10 fs, the slowly varying envelope approximation starts to break down and the formalism of this paper is no longer valid.

We proceed with a brief discussion of several second order effects. In the numerical examples of this paper, there is a photoionization process of ⁸⁷Rb due to three photon absorption of the strong switching beam. In crystal experiments [18], these free electrons cause attenuation of the probe beam on longer time scales (10 ps–1 ns) and therefore cause an undesired slow response of the medium on top of the fast switching response. We have estimated the densities of generated free electrons due to the three photon absorption of the

switching laser beam for the numerical simulations of Fig. 2. We have found the absorption of the probe beam due to these free electrons to be negligible. As a result, the medium should not have significant slow response on top of the fast switching response. Another concern is the nonlinear self-focusing or defocusing of the strong switching beam while propagating through the atomic vapor cell. For the numerical simulations of Figs. 2–4, we calculate the nonlinear index for the atomic medium to be $n_2 = 7.8 \times 10^{-8}$ cm²/GW. This nonlinear index causes a nonlinear phase shift of about $\pi/10$ at the intensity peak of the switching beam at the end of the atomic vapor cell. We therefore do not expect any significant change in the spatial beam profile of the strong switching laser for the numerical simulations of Figs. 2–4. Finally, our scheme requires vapor cell densities on the order of $N = 10^{15}$ /cm³. For these densities, the average collision time for an atom is many nanoseconds which is much larger than the switching time scale. As a result, we do not expect collisional processes between atoms to be of importance.

In conclusion, we have suggested a scheme that performs all optical switching in femtosecond time scales. One advantage of using ⁸⁷Rb is the convenience of the transition wavelengths. The experiment of Fig. 2 will require a Ti:sapphire femtosecond laser at a wavelength of 780 nm and a fiber laser at a wavelength of 1.5 μ m. Although throughout this paper we have focused on the switching application, we expect our scheme to also be able to produce shaped pulses at the probe wavelength by using shaped femtosecond switching pulses.

The author would like to thank Alexei Sokolov, Thad Walker, Marie Delaney, Todd Johnson, Erich Urban, and Hilmi Volkan Demir for helpful discussions. This work was partially supported by a start-up grant from the Department of Physics at University of Wisconsin-Madison.

-
- [1] G. Steinmeyer, *J. Opt. A, Pure Appl. Opt.* **5**, 1 (2003).
 - [2] E. P. Ippen and C. V. Shank, *Appl. Phys. Lett.* **26**, 92 (1975).
 - [3] N. Sugimoto, S. Ito, S. Fujiwara, T. Suzuki, H. Kanbara, and K. Hirao, *Opt. Commun.* **161**, 47 (1999).
 - [4] B. L. Yu, A. B. Bykov, T. Qiu, P. P. Ho, R. R. Alfano, and N. Borrelli, *Opt. Commun.* **215**, 407 (2003).
 - [5] S. Pereira, P. Chak, and J. E. Sipe, *Opt. Lett.* **28**, 444 (2003).
 - [6] M. J. LaGasse, K. K. Anderson, H. A. Haus, and J. G. Fujimoto, *Appl. Phys. Lett.* **54**, 2068 (1989).
 - [7] J. S. Aitchison, A. Villeneuve, and G. I. Stegeman, *Opt. Lett.* **18**, 1153 (1993).
 - [8] E. J. Gansen, K. Jarasiunas, and A. L. Smirl, *Appl. Phys. Lett.* **80**, 971 (2002).
 - [9] M. Gicquel-Guezo, S. Loualiche, J. Even, C. Labbe, O. Dehaese, A. L. Corre, H. Folliot, and Y. Pellan, *Appl. Phys. Lett.* **85**, 5926 (2004).
 - [10] W. J. Johnston, M. Yildirim, J. P. Prineas, A. L. Smirl, H. M. Gibbs, and G. Khitrova, *Appl. Phys. Lett.* **87**, 101113 (2005).
 - [11] M. B. Yairi, H. V. Demir, and D. A. B. Miller, *Opt. Quantum Electron.* **33**, 1035 (2001).
 - [12] J. H. Wu, J. Y. Gao, J. H. Xu, L. Silvestri, M. Artoni, G. C. LaRocca, and F. Bassani, *Phys. Rev. Lett.* **95**, 057401 (2005).
 - [13] N. S. Patel, K. L. Hall, and K. A. Rauschenbach, *Appl. Opt.* **37**, 2831 (1998).
 - [14] M. Scalora, J. P. Dowling, C. M. Bowden, and M. J. Bloemer, *Phys. Rev. Lett.* **73**, 1368 (1994).
 - [15] A. Hache and M. Bourgeois, *Appl. Phys. Lett.* **77**, 4089 (2000).
 - [16] M. Naruse, H. Mitso, M. Furuki, I. Iwasa, Y. Sato, S. Tatsuura, and M. Tian, *Opt. Lett.* **29**, 608 (2004).
 - [17] X. Hu, Y. Liu, J. Tian, B. Cheng, and D. Zhang, *Appl. Phys. Lett.* **86**, 121102 (2005).
 - [18] O. Beyer, D. Maxein, K. Buse, B. Sturman, H. T. Hsieh, and D. Psaltis, *Phys. Rev. E* **71**, 056603 (2005).
 - [19] M. S. Safronova, C. J. Williams, and C. W. Clark, *Phys. Rev. E* **69**, 022509 (2004).